Nonphotochemical Quenching of Excitation Energy in Photosystem II. A Picosecond Time-Resolved Study of the Low Yield of Chlorophyll *a* Fluorescence Induced by Single-Turnover Flash in Isolated Spinach Thylakoids†

Sergej Vasil'ev‡,§ and Doug Bruce*,‡

Department of Biological Sciences, Brock University, St. Catharines, Ontario, L2S 3A1, Canada, and Department of Biology, M.V. Lomonosov, Moscow State University

Received March 25, 1998; Revised Manuscript Received May 28, 1998

ABSTRACT: Chlorophyll *a* fluorescence emission is widely used as a noninvasive measure of a number of parameters related to photosynthetic efficiency in oxygenic photosynthetic organisms. The most important component for the estimation of photochemistry is the relative increase in fluorescence yield between dark-adapted samples which have a maximal capacity for photochemistry and a minimal fluorescence yield (F_0) and light-saturated samples where photochemistry is saturated and fluorescence yield is maximal (F_m). However, when photosynthesis is saturated with a short (less than 50 μs) flash of light, which induces only one photochemical turnover of photosystem II, the maximal fluorescence yield is significantly lower (F_{sat}) than when saturation is achieved with a millisecond duration multiturnover flash (F_m). To investigate the origins of the difference in fluorescence yield between these two conditions, our time-resolved fluorescence apparatus was modified to allow collection of picosecond time-resolved decay kinetics over a short time window immediately following a saturating single-turnover flash (F_{sat}) as well as after a multiturnover saturating pulse (F_m). Our data were analyzed with a global kinetic model based on an exciton radical pair equilibrium model for photosystem II. The difference between F_m and F_{sat} was modeled well by changing only the rate constant for quenching of excitation energy in the antenna of photosystem II. An antenna-based origin for the quenching was verified experimentally by the observation that addition of the antenna quencher 5-hydroxy-1,4-naphthoquinone to thylakoids under F_m conditions resulted in decay kinetics and modeled kinetic parameters very similar to those observed under F_{sat} conditions in the absence of added quinone. Our data strongly support the origin of low fluorescence yield at F_{sat} to be an antenna-based nonphotochemical quenching of excitation energy in photosystem II which has not usually been considered explicitly in calculations of photochemical and nonphotochemical quenching parameters. The implications of our data with respect to kinetic models for the excited-state dynamics of photosystem II and the practical applications of the fluorescence yield parameters F_m and F_{sat} to calculations of photochemical yield are discussed.

In photosynthetic organisms, a change of actinic light intensity results in a complex time course of changing chlorophyll *a* (Chl *a*) fluorescence yield. Numerous processes contribute to these kinetics, making them a rich source of information about photosynthetic mechanisms and their regulation. The potential information content and the noninvasive nature of fluorescence analysis have made variable Chl *a* fluorescence one of the most widely used techniques for the evaluation of numerous photosynthetic parameters. Many of these parameters are directly related to photosystem II (PS II)[1] which is the source of almost all of the Chl *a* fluorescence observed at room temperature. Some of the PS II associated parameters determined from studies of fluorescence yield are photochemical efficiency (*1*−*3*), functional absorption cross section (*4*−*7*), kinetics of electron transfer on the acceptor side (*8*, *9*), and the capacity of the electron donor side (*10*, *11*). In addition, studies of Chl *a* fluorescence decay kinetics on a picosecond time scale have provided insight into the fundamental molecular mechanisms of energy conversion in PS II (*12*−*15*).

Measurements of the degree of quenching of Chl *a* fluorescence by both photochemical processes and nonphotochemical processes are critical to the determination of the above-mentioned PS II associated parameters. Measures of photochemical quenching are routinely made by quantifying the increase in fluorescence observed upon light-induced

† Supported by operating and equipment grants from the Natural Sciences and Engineering Research Council of Canada (NSERC) to D.B.

* Address correspondence to this author at the Department of Biological Sciences, Brock University, St. Catharines, Ontario, Canada L2S 3A1. Telephone: (905) 688-5550, ext 3826. FAX: (905) 688-1855. E-mail: dbruce@spartan.ac.brocku.ca.

‡ Brock University.

§ Moscow State University.

[1] Abbreviations: PS, photosystem; PQ, plastoquinone pool; RP, radical pair; RRP, reversible radical pair; F_0, minimal fluorescence yield; F_m, maximal fluorescence yield; F_{sat}, maximal fluorescence yield induced by single-turnover flash; F_v, $F_m - F_0$; Q_A, primary quinone acceptor of photosystem II; DAS, decay-associated spectrum; Pheo, pheophytin; 5-OH-NQ, 5-hydroxy-1,4-naphthoquinone.

S0006-2960(98)00685-0 CCC: $15.00
Published on Web 07/17/1998

saturation of PS II photochemistry. The kinetics of fluorescence induction from the initial fluorescence level F_0 (maximal photochemistry) to the maximum fluorescence level F_m (light-saturated photochemistry) after the rapid onset of continuous light follow a complex polyphasic pattern with two intermediate states. These transients are usually addressed as O-J-I-P (*16, 17*) or F_0- I_1-I_2 -F_m (*18, 19*), and they indicate clearly two well-separated parts, the so-called photochemical and thermal phases of fluorescence induction. The fast phase of fluorescence rise from the minimal fluorescence level F_0 to the J level follows the reduction of the primary quinone electron acceptor of PSII (Q_A) and has thus been called the photochemical phase. This phase is limited by the absorption of excitation energy and the rate of Q_A reduction; it can be finished in about 50 μs. The remaining part of the fluorescence rise from J to the maximal level F_m (thermal phase) is relatively slow and requires about 100 ms to be completed (20).

Another experimental approach to study fluorescence increases induced by actinic light is the pump−probe fluorescence method introduced by Mauzerall (*4*). In this technique, fluorescence yield is measured with a weak probe pulse after a variable intensity actinic pump flash. The yield determined with probe flash alone is equivalent to the F_0 level, and the maximum yield attained by the probe flash after a saturating single-turnover pump flash (F_{sat}) is very similar in magnitude to the J level discussed above. The F_{sat} level is considerably lower than the F_m level when short-duration "single turnover" pump flashes are used. It has been demonstrated that pump flashes longer than about 50 μs (*21, 22*) and/or the addition of a background illumination (*23*) are required to induce higher fluorescence yields similar to the F_m level observed under continuous illumination.

It is clear that two distinct components contributing to the fluorescence yield of light-saturated PS II centers can be observed by both fluorescence induction and flash saturation techniques. The typical relative fractional amplitudes of the "photochemical" and "thermal" phases measured with either technique are about 60% and 40%, respectively. The mechanism responsible for these two phases of fluorescence increase is still a matter of debate (*21, 22, 24*−*27*). It has been suggested that an oxidized nonphotochemical quencher which is gradually reduced in the course of multiple-turnover excitation of PS II is responsible for the low F_{sat} yield (*24*). Several hypotheses have been proposed to account for the origin of this quencher: oxidized plastoquinone molecules (*25*), alternative quencher Q_2 (*26, 27*), multiple structurally independent quenchers (*21, 22*). Alternatively, the difference in F_{sat} and F_m has been suggested to arise from variations in the yield of recombination fluorescence in closed PS II reaction centers (*28*). F_m is used almost exclusively in calculations of quantum yield or photosynthetic efficiency and in calculations of photochemical and nonphotochemical quenching of fluorescence, even though the origin of the high yield of fluorescence after multiple turnovers of PS II is still under debate. In view of the wide use of variable fluorescence in photosynthesis research, a clarification of the origins of F_m and F_{sat} is of importance.

Molecular mechanisms underlying the fluorescence induction pattern are based on the dynamics of primary radical pair reactions in PS II. Steady-state fluorescence measurements provide only limited information as they do not allow a clear distinction as to which of the individual reactions within PS II are affected in the course of the F_0 to F_{sat} to F_m transitions. A number of studies have measured picosecond fluorescence decay kinetics and successfully applied the reversible radical pair (RRP) model to investigate primary photochemical processes in photosynthetic reaction centers (*29*) and to describe excitation energy transfer and trapping in PS II (*30*−*34*). However, all previous studies of PS II have examined only the two extreme fluorescence states corresponding to the F_0 and F_m levels. The implicit assumption shared by these investigations was that only photochemistry contributed to the difference between F_0 and F_m levels. Picosecond fluorescence decay kinetics have never been measured at F_{sat}, and thus the thermal phase has never been considered explicitly.

What is the functional difference between PS II reaction centers closed by a single-turnover pulse of saturating light and those exposed to multiple turnovers? What are the origins of F_{sat} and F_m, and how do they relate to the RRP model of PS II? Finally, based on answers to the previous questions, which level (F_{sat} or F_m) is appropriate to determine photochemical and nonphotochemical quenching parameters, quantum yield, and photosynthetic efficiency?

In this contribution, we describe an experimental technique for the measurement of fluorescence decay kinetics at the F_{sat} level and analyze decay-associated spectra gathered from thylakoid membranes at F_0, F_{sat}, and F_m levels with the RRP kinetic model. Our results provide strong evidence for an antenna quenching mechanism as the origin of the low fluorescence yield at F_{sat} and thus provide a theoretical basis for the use of F_{sat} rather than F_m in calculations of photochemical quenching parameters.

MATERIALS AND METHODS

Thylakoids were isolated from market spinach as described in Whitmarsh and Ort (*35*) and stored at −80 °C at a concentration of about 2 mg of Chl/mL. For measurements, the thylakoids were diluted in buffer (0.3 M sorbitol, 10 mM Hepes, 4 mM $MgCl_2$, 0.5 g/L BSA, pH 7.5) to a final concentration of 5 μg of Chl/mL. Chlorophyll concentrations were measured according to Zeigler and Egle (*36*).

Fluorescence decay kinetics were measured with the single photon timing apparatus described previously (*11*). The sample was excited at 665 nm by 60 ps laser pulses delivered by a Hamamatsu picosecond diode laser (PLP-01) set to 10 MHz repetition rate. Part of the excitation pulse reflected from a glass plate was focused onto a fast avalanche photodiode used as the timing reference. Fluorescence emission was detected by a Hamamatsu R-2809 microchannel plate photomultiplier screened by a double monochromator. This yielded an instrument response function of about 70 ps. Instrument response functions were collected as background decay from cold, circulating water at 665 nm. Fluorescence decays were recorded between 680 and 730 nm (8 detection wavelengths) with 50 000 counts in the peak channel.

The samples (500 mL, 5 μg of Chl/mL) were kept in the dark and pumped with a flow speed of about 400 mL/min through a laboratory-built nozzle forming a 1 mm diameter jet used as the measurement area for detection of fluorescence. This allowed the preparation to remain at F_0 with

open reaction centers. To induce F_{sat}, a small piece of the jet (2 mm long) was illuminated by an actinic single-turnover light flash delivered by a diode laser (wavelength 665 nm, 300 mW; RPMC Inc.) operating in pulsed mode (30 μs rectangular pulse). The picosecond pulsed measuring beam was aimed at the leading edge of the illuminated piece of jet. The image field of the collimating detection optics used to deliver fluorescence to the emission monochromator was 0.5 mm. The input slit of the monochromator was physically screened during actinic diode laser flash by an optical chopper running at a frequency of 4.2 kHz (50% duty cycle). The laser diode driver was synchronized with the chopper such that the input slit of the monochromator was exposed to fluorescence from the sample 2 μs after the saturating 30 μs flash for a time interval of 100 μs.

The two key requirements of this continuous flow configuration were that fluorescence was collected from sample which had previously been illuminated by the actinic diode laser flash and that the sample volume was exchanged completely between saturating flashes. To allow more control over the timing of data acquisition, the time to amplitude converter was synchronously gated which allowed variation in both the time delay between the saturating flash and data collection window and the total duration of the window itself. Typically, data were collected over a time window from 30 to 65 μs after the actinic diode laser flash.

The F_m state was achieved with the same circulating system described above by illuminating samples with saturating light in a preillumination chamber of 2 mL volume located just before the sample jet. The samples were thus exposed to saturating light for 300 ms just prior (less than 3 ms) to measurement.

In all experiments, the bulk of the 500 mL samples was kept on an ice bath during measurement to avoid destabilization of the thylakoids. Effects of aging were not detected during the collection of data sets as judged from comparison of decay kinetics measured at the same wavelength at the beginning and the end of each experiment.

The fluorescence decay curves from all detection wavelengths were fit simultaneously using one of two different global model functions: a sum of five exponential decay components and the RRP model (*29*). For details of the laboratory written software used for all kinetic modeling, please contact S. Vasil'ev.

Pump−probe measurements of the fluorescence yield were carried out as described previously (*11*) using actinic light flashes (250 ns fwhm) generated by a Phase-R DL-32 dye laser operating at 650 nm and a weak Xenon flash lamp as probe. Some comparative measures of fluorescence yield were also obtained with a pulse amplitude modulated (PAM) fluorometer (Walz, Germany).

RESULTS AND DISCUSSION

An Introduction to the Experimental Technique. First of all, we show that using our technique, developed for picosecond kinetic measurements, we are able to observe the same three fluorescence states (F_0, F_{sat}, and F_m) that are observed with a conventional pump−probe apparatus. A typical single-turnover flash saturation curve obtained using the single photon timing technique (30 μs actinic light pulses) is shown in Figure 1 with the best fit to the data set using

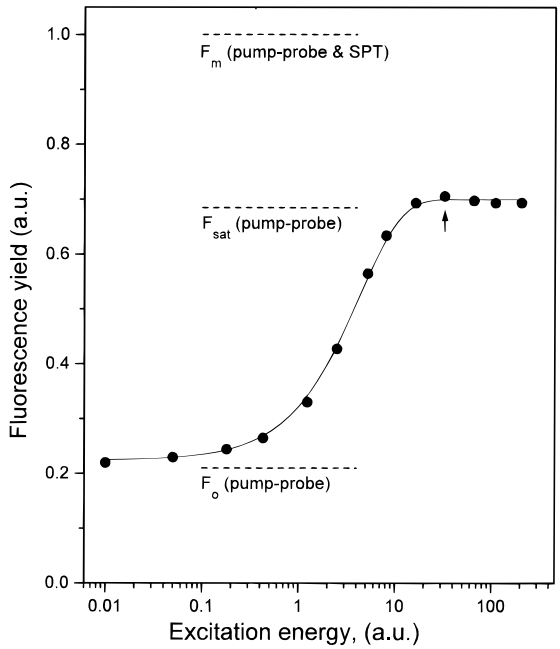

FIGURE 1: Flash saturation curve of variable chlorophyll fluorescence yield of thylakoid membranes measured with the single-photon timing technique using 30 μs actinic flashes (see Materials and Methods). The Chl concentration was 5 μM. The dashed lines show F_0, F_{sat}, and F_m levels measured with a traditional pump−probe apparatus (see Materials and Methods for details). F_0 and F_m levels measured with a pulse amplitude modulated (PAM) fluorometer were identical to the F_0 and F_m levels shown for the pump−probe technique.

the single-hit Poisson distribution. The total fluorescence yield arising from measuring the picosecond light pulses increased from a minimal fluorescence yield (F_0) at low actinic light intensities (all PS II centers open) to a maximal fluorescence yield (F_{sat}) obtained with saturating pump flash intensities (all PS II centers closed). This result shows that the intensity of our actinic light pulse was sufficient for complete closure of all PS II reaction centers under single-turnover conditions. As described under Materials and Methods, the actinic pulse duration used for collection of this data set was 30 μs. Very similar curves were obtained when the width of the actinic diode laser pulse was varied from 15 to 50 μs (data not shown). For all subsequent fluorescence decay measurements at the F_{sat} level, the intensity of the actinic light pulses was set above the saturation level and is shown by the arrowhead in Figure 1. The F_m level detected by the single photon timing technique is also shown in Figure 1. As described under Materials and Methods, the samples were exposed to 300 ms of saturating light just prior to measurement, conditions sufficient to induce multiple turnovers of PS II. The maximum Chl *a* emission yield induced by a single-turnover saturating flash (F_{sat}) was clearly lower than that observed under saturating multiturnover light flashes (F_m). For comparison, Figure 1 also shows the corresponding fluorescence yields at F_0, F_{sat}, and F_m obtained from independent pump−probe measurements with single-turnover (250 ns) actinic light pulses. To achieve F_m values with the pump−probe spectrometer, a saturating background blue light was shone on the sample during the measurement as described previously (*23*). A very strong correlation between F_m, F_{sat}, and F_0 yields, measured with the two techniques is clearly evident.

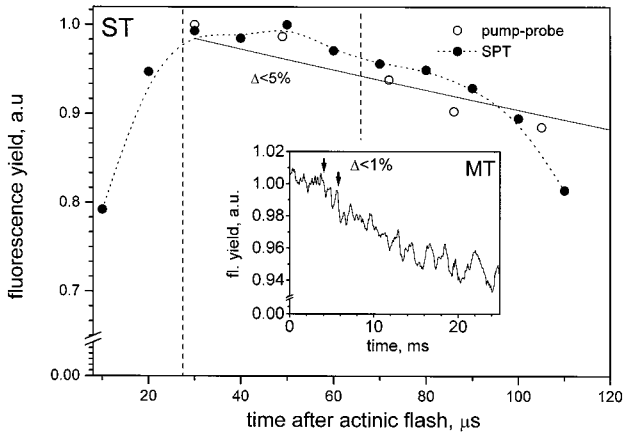

FIGURE 2: Variable fluorescence relaxation kinetics (microsecond time scale) measured after saturating single-turnover flash excitation by both the single photon timing (SPT) and pump−probe techniques. The inset shows the relaxation kinetics of variable fluorescence after a multiple-turnover (300 ms) saturating flash as measured with the PAM fluorometer.

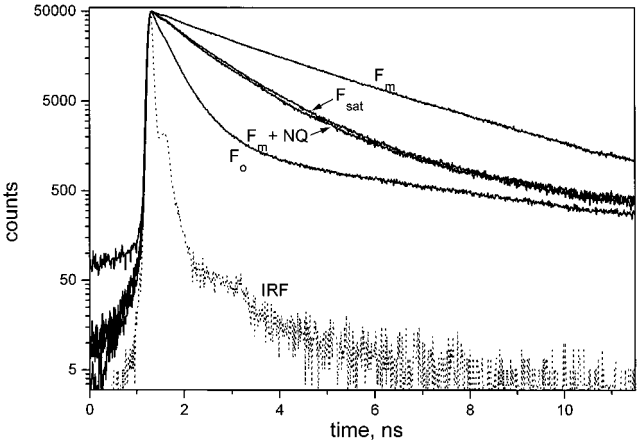

FIGURE 3: Fluorescence decay kinetics of spinach thylakoids at F_0, F_{sat}, F_m, and $F_m^{[Q]}$ with the addition of 15 μM 5-OH-NQ. The instrument response function is also shown.

Both techniques, showed an F_v/F_0 ratio of about 3.5 (where $F_v = F_m - F_0$), and as shown previously (*23*), F_m was about 30% higher than F_{sat}. In addition, a F_v/F_0 of 3.5 was also obtained with the samples measured with a conventional pulse amplitude modulated (PAM) fluorometer using 300 ms saturating light flashes (data not shown).

In the present study, we investigated energy conversion in thylakoid membranes with minimally modified reaction centers. No modifying chemical agents were used to block electron transfer and/or to stabilize the F_m state. PS II was "closed" (primary quinone electron acceptor Q_A reduced) only by exposure to saturating light. Two general problems arise when actinic light alone is used to close reaction centers: (i) relaxation of the closed state owing to the time delay between excitation with the saturating light and measurement; (ii) possible limitations on the donor side. Therefore, it remained to be shown how closely we were able to approach F_m and F_{sat} with fully reduced Q_A.

To address this question, the relaxation kinetics of variable fluorescence were measured after single-turnover and multiple turnover flashes and are shown in Figure 2. The time course of the F_{sat} yield measured with the single photon timing system exhibits a steep rise at a time interval of 0−30 μs after the actinic flash and a steep decay at 100−120 μs. This pattern originates from the exposure and screening of the detection monochromator by the optical chopper. In the time window from 30 to 100 μs, the fluorescence yields measured by single photon timing and pump−probe techniques were indistinguishable, and the decrease of the fluorescence yield over the detection time window was less than 5%. The inset in Figure 2 shows the millisecond time course of F_m decay measured after a 300 ms multiturnover flash with a PAM fluorometer. In the case of multiturnover excitation, the decrease of the fluorescence yield from its maximal value to that at the moment of measurement (3 ms after the pulse) was less than 1%.

To summarize: testing of the developed instrumentation showed excellent correspondence between the single photon timing, pump−probe, and PAM techniques and thus indicates the ability to accurately measure picosecond fluorescence decay kinetics at F_0, F_{sat}, and F_m.

Fluorescence Decays. Typical fluorescence decay kinetics of spinach thylakoids for F_0, F_{sat}, and F_m states measured at 685 nm using the above-described techniques are shown in Figure 3. Decays measured at F_{sat} contained a small fraction (about 0.1%) of background fluorescence, clearly observed before the excitation pulse. This feature originates from delayed fluorescence, and in the fitting procedure, it was modeled by a background, constant over the time window of measurement. The fluorescence decay measured at F_{sat} was considerably faster than at F_m. The addition of 5-OH-NQ (final concentration, 15 μM) to samples under F_m conditions resulted in an acceleration of the decay kinetics so they were almost identical to those obtained at F_{sat}.

Global Lifetime Analysis. Fluorescence decay curves were recorded for eight detection wavelengths between 680 and 730 nm. The fluorescence decay data were analyzed globally by fitting to a sum of exponential decays to obtain lifetimes and corresponding decay-associated spectra (DAS) (*37*). Considering the weighted residuals, autocorrelation plots, and values of χ^2, it was found that a sum of five exponentials was necessary to fit the data at all three states. This is in agreement with previous studies on pea thylakoids at F_0 and F_m (*30, 31*).

The DAS corresponding to measurement conditions F_0, F_{sat}, and F_m are shown in Figure 4. In all conditions, the fastest DAS component had a lifetime $\tau_1 = 11-15$ ps and was attributed to exciton equilibration within the antenna complexes. Also observed in all conditions was the DAS of the second lifetime component ($\tau_2 = 70-125$ ps) which peaked at about 690 and 720 nm and was assigned mainly to PS I emission. The amplitude of the second lifetime component around 690 nm was decreased relative to the band at 720 nm upon transition from F_0 to F_m. This feature was observed in a previous study and proposed to originate from a better separation of fast PS I decay components after PS II decay kinetics were slowed by PS II closure (*30*). The two fast decay components (characterized by τ_1 and τ_2) were found in all measuring conditions in approximately the same proportion.

The third and the fourth decay components at F_0 ($\tau_3 =$ 245 and $\tau_4 = 515$ ps) had similar DAS peaking around 685 nm and only minor emission at longer wavelengths and were assigned to PS II. The fifth component (τ_5 about 4 ns) had

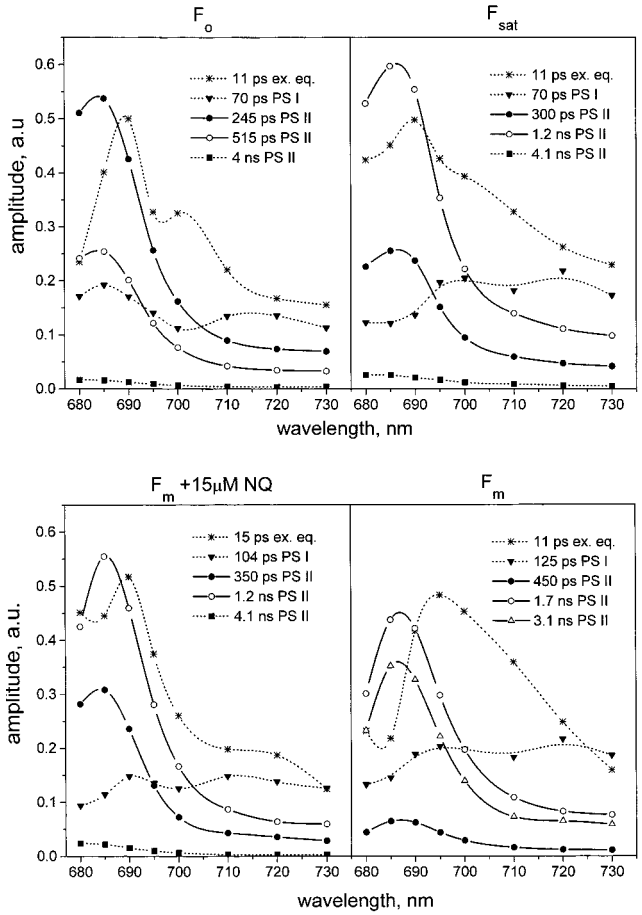

FIGURE 4: Decay-associated spectra of spinach thylakoids at F_0, F_{sat}, F_m, and $F_m^{[Q]}$ with addition of 15 μM 5-OH-NQ, as calculated from the amplitudes of the five components used in the global lifetime analysis of the fluorescence decay kinetics (see Materials and Methods for details). All DAS are normalized at 685 nm to the sum of all decay components (except exciton equilibration).

a very small relative amplitude and was assigned to a small fraction of PS II with closed reaction centers. The DAS for F_{sat} showed two PS II associated components (lifetimes of 300 and 1.2 ps) whereas the measuring condition F_m was characterized by DAS with three PS II components (lifetimes of 450 ps, 1.7 ns, and 3.1 ns). The increased fraction of the slow decay component at F_{sat} compared to F_0 was assigned to a small fraction of PS II in state F_m which appeared under these conditions.

The DAS at F_0 was almost identical to those reported previously. The DAS obtained for F_m qualitatively resembles results of the previous reports (*30*, *31*), but the relative amplitude and lifetime of the fast PS II component ($\tau = 450$ ps) found in our study were somewhat smaller. This is correlated with a larger F_m/F_0 in our samples (6.2) compared to previous reports (4.9) as calculated from the ratio of the sum of amplitudes of all PS II components in F_m and F_0. A number of factors may have contributed to this difference. The maximal fluorescence yield in earlier fluorescence decay studies was achieved by inhibition of PS II by DCMU rather than by light saturation alone. The delay time between saturating light exposure and fluorescence decay detection was considerably longer in previous studies than in the present study (3 ms). However, the difference most likely arises from variation in sample preparations. Due to the strong correlation between the F_m/F_0 observed between our

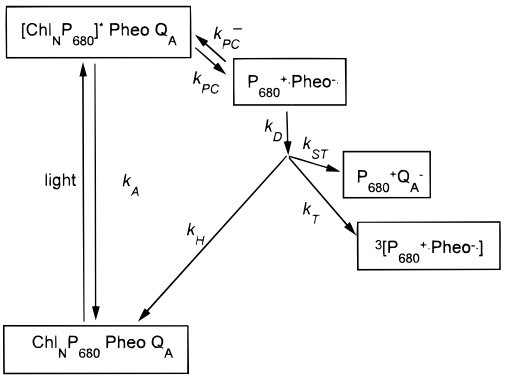

FIGURE 5: Reversible radical pair model for primary processes in PS II (29; 51). $[Chl_N P_{680}]^*$ symbolizes the exciton equilibration among N antenna Chl molecules and P680. The rate constants describe excitation decay from the antenna (k_A), the primary charge separation (k_{PC}), and its reversal (k_{PC}^-). The rate constant for decay of the primary radical pair (k_D) is the sum of the rate constants of charge stabilization by electron transfer from $Pheo^{-\bullet}$ to Q_A (k_{ST}), triplet formation (k_T), and heat loss (k_H).

single photon timing, pump−probe, and PAM studies, we are confident that we have achieved a true F_m.

The major changes in DAS upon closure of reaction centers by single-turnover flashes occurred in the amplitudes and lifetimes of the two PS II components observed at F_0 and F_{sat} (Figure 4). The 245 ps component dominating the PS II associated DAS at F_0 was replaced by the 1.2 ns component which dominated the PS II contribution to F_{sat}. The changes in DAS between F_0 and F_{sat} are less complex than those between F_0 and F_m. This is consistent with the idea that F_{sat} reflects only a photochemical event and F_m both a photochemical and the so-called "thermal" phase of fluorescence yield increase.

The major difference between the F_{sat} and F_m states is the large contribution by the 3.1 ns PS II associated component to F_m which is not present at F_{sat}. Interestingly, the DAS observed under F_m conditions in the presence of the antenna quencher 15 μM 5-OH-NQ was very similar to that obtained at F_{sat}.

Kinetic Analysis. To reveal the molecular mechanisms which give rise to the changes between F_{sat} and F_m, we applied the RRP model (*29*) to analyze our data. A simplified kinetic pattern of the RRP model used is shown in Figure 5. According to this model, PS II is characterized by a set of rate constants (k_A, k_{PC}, k_{PC}^-, k_D) and by an amplitude factor, which is proportional to the number of Chls functionally connected to PS II. To account for the fluorescence decay components not associated with PS II (PS I and exciton equilibration), two exponential components with parameters A_i and τ_i were added to the kinetics of the model.

A previous detailed study on the fluorescence decay kinetics of pea thylakoids at F_0 and F_m led to the conclusion that PS II emission is heterogeneous (*30*). However, in this earlier study a substantial improvement of the fit quality over that obtained with a homogeneous PS II model was observed only in combined global analysis of decay kinetics measured at F_0 and F_m. When analyzed separately, fluorescence decays at F_0 were well described in that study by assuming a homogeneous PS II characterized by a biexponential decay with lifetimes of 290 and 630 ps. In view of the complexity

Table 1: Results from Global Target Kinetic Analysis of the Fluorescence Decay of Spinach Thylakoids at F_0, F_{sat}, F_m, and $F_m^{[Q]}$ States[a]

condition	rate constants, ns^{-1}			
	k_A	k_{PC}	k_{PC}^-	k_D
F_0	**0.83**	**2.6**	**0.39**	**2.2**
F_0	0.3	3.1	0.35	2.4
F_{sat}	**0.83**	**0.5**	**1.2**	**0.8**
F_{sat}	0.3	1.0	0.56	1.42
$F_m^{[Q]}$	**0.83**	**0.42**	**0.9**	**0.89**
$F_m^{[Q]}$	0.3	0.93	0.42	1.42
F_m ($\alpha/\beta = 1$), α	0.3	0.7	1.6	1.9
F_m ($\alpha/\beta = 1$), β	0.3	0.5	2.6	0.46
F_m ($\alpha/\beta = 2$), α	0.3	0.6	1.1	1.4
F_m ($\alpha/\beta = 2$), β	0.3	0.02	—[b]	—[b]

[a] The results from the target analysis with different fixed values for k_A are shown. Target analysis for the F_m condition was performed assuming a heterogeneous PS II model; accordingly, two sets of rate constants are shown for this case. Boldface numbers represent the sets of the rate constants, calculated with $k_A = 0.83$. χ^2 values generated for fits ranged between 0.99 and 1.23. [b] Rate constants are not shown owing to the large error in estimation of these parameters which results from the very small value for k_{PC}.

of kinetics in our results and in the previous work done at F_m, we analyzed our data with both homogeneous and heterogeneous PS II models. Despite the high signal/noise ratio of the data collected in the present study (50 000 counts in the peak channel), we found no substantial improvement of the fit quality at either F_0 or F_{sat} when the heterogeneous PS II model was applied.

Only three rate constants of four can be independently determined from the fluorescence data. Kinetic modeling performed in previous studies assumed that the rate constant for excitation decay in the antenna (k_A) was equal for both F_0 and F_m states and was usually set to a value of 0.3 ns^{-1}, which corresponds to a fluorescence lifetime of the (hypothetical) isolated light-harvesting antenna complex of 3.3 ns (*38*). This approach is not well justified as the reduction of the plastoquinone pool and/or the putative quencher Q_2 upon transition from the F_0 to F_m state is likely to eliminate at least some nonphotochemical antenna-based quenching (*25, 39*). Rate constants for the RRP model are rather robust to any variations in k_A at F_0 owing to the fast electron transfer from $Pheo^{-\bullet}$ to Q_A, but as reaction centers are closed, this model becomes more sensitive to small variations in k_A. We propose that it is more reasonable to assume that the F_{sat} and F_0 states are characterized by equal k_A values and therefore performed a combined global target analysis of the kinetics at F_0 and F_{sat} with a homogeneous RRP model (Figure 5). For this analysis, k_A was first set to 0.3 ns^{-1}, and the following three constraints were applied: the lifetimes for exciton equilibration, PS I emission, and the lifetime of the slowest decay component were set to be the same for F_0 and F_{sat}. These minimal constraints are reasonable and were expected to lead to better separation of PS II decay components. Optimal values for the rate constants of PS II resulting from kinetic modeling are shown in Table 1. The values of the rate constants obtained for F_0 ($k_{PC} = 3.1$ ns^{-1}, $k_{PC}^- = 0.35$ ns^{-1}, $k_D = 2.4$ ns^{-1}) are in good agreement with previous studies (*30, 31, 37*). As expected for the F_{sat} state, we observed a decrease in k_{PC} and in k_D accompanied by an increase in k_{PC}^-.

In contrast to F_0 and F_{sat}, the PS II emission at F_m was complex and no longer could be described by a homogeneous model with the same constraints described above. Finding a unique solution for all rate constants of a heterogeneous PS II model from fluorescence data alone is impossible as parameters of the model depend on the relative amount of two types of PS II. Thus, determination of the total amount of chlorophyll molecules, associated with each of the two types of PS II, is required to solve this problem.

Numerous studies have investigated the heterogeneity among PS II centers [reviewed in (*40*)]. Analysis of fluorescence induction data has been proposed to reveal the presence of two distinct populations of PS II (named α and β) which differ in their rate of Q_A^- formation. The fraction of the slow (PS IIβ) centers has been calculated to be 20−30% of the total amount (*41*). A significant fraction of PS II reaction centers (about 30%) have been found to be photochemically competent but inactive in PQ reduction (*42*). There are a number of features common to PQ-nonreducing centers and PS IIβ, but strict identity between them does not always hold (*40*). It has been suggested that the PQ-nonreducing centers are a subpopulation of PS IIβ centers. PS II centers differ also in antenna size, antenna protein composition (*43*), and susceptibility to photoinhibition (*44*).

It is still unclear how all of these differing manifestations of PS II heterogeneity are related to excited-state dynamics and picosecond decay kinetics. Two previous detailed time-resolved fluorescence studies led to quite different conclusions concerning the assumed number of emitting Chls coupled to PS IIβ (*30, 31*).

To be independent of any assumptions concerning PS IIβ content in our samples we analyzed F_m data with the heterogeneous PS II model using different fixed PS IIα/PS IIβ ratios. It was found that our data could be described well by the model without loss of fit quality if the PS IIα/PS IIβ ratio was in the range of 1.0−2.4. Table 1 presents PS II rate constants derived from the kinetic analysis of F_m for PS IIα/PS IIβ ratios at two extremes of this range, 1.0 and 2.0. At a PS IIα/PS IIβ of 1.0, unique solutions for all rate constants in both types of centers are clearly observed, and both centers would contribute biexponential decay kinetics to the fluorescence decay. This kind of result was obtained in one of the previous studies of PS II excited state dynamics where a relatively large amount (34%) of all emitting Chls was assumed to be associated with PS IIβ (*30*). In our study, as PS IIα/PS IIβ increases to 2 and beyond, we found that k_{PC} for the PS IIβ centers tended to zero and the errors associated with k_{PC}^- and k_D increased dramatically. Under these conditions, the kinetics for PS IIβ centers are defined almost entirely by k_A. These PS II centers (inactive in PQ reduction) would contribute a primarily monoexponential decay of approximately 3 ns lifetime to the DAS for F_m as was observed in our exponential decay analysis and shown in Figure 4. A similar "simplification" of the heterogeneous model was used in one of the other previous kinetic studies of heterogeneity which assumed a relatively small amount (23%) of emitting Chls associated with PS IIβ centers (*31*). The idea that the origin of heterogeneity arises from centers where k_{PC} is very low is supported by flash yield studies which have indicated that approximately 30% of PS II centers are essentially inactive in electron transport to plastoquinone (*42*).

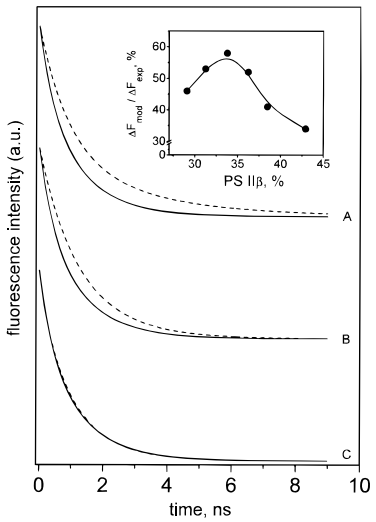

FIGURE 6: Calculated PS II fluorescence decay curve obtained from the global target analysis of experimental data at F_{sat} (solid lines), compared to the respective model curves (dashed lines) obtained by changing of rate constants in the kinetic model for F_m shown in Figure 5. Complete elimination of recombination fluorescence by increasing k_D to a very large value or by setting k_{PC}^- to zero if PS IIα/PS IIβ = 0.8 (A); the same changes in rate constants as for the previous case, but PS IIα/PS IIβ = 2 (B); k_A = 0.83 (PS IIα/PS IIβ = 0.8) or k_A^α = 0.83, k_A^β = 0.79 (PS IIα/PS IIβ = 2) (C). The inset shows the relative part of the fluorescence yield increase, that cannot be described by recombination fluorescence: $(F_{model} - F_{sat})/(F_m - F_{sat})$, where F_{model} is the fluorescence yield calculated from the set of the rate constants for F_m, modified as in panels A and B, as a function of PS IIβ fraction. Please see the text for additional details.

Testing Hypotheses for the Origin of the "Thermal Phase". Determination of the PS II rate constants enabled us to test various hypotheses suggested to account for the difference in fluorescence yield between F_m and F_{sat}. Several possible origins of the fluorescence quenching at F_{sat} have been previously suggested: (i) oxidizing equivalents on the donor side of PS II (*45*), (ii) oxidized non-heme iron of PS II (*46*), (iii) oxidized plastoquinone pool and/or an unidentified quencher, Q_2 (*25*−*27*), and (iv) decrease of the yield of recombination fluorescence caused by a transiently enhanced rate of the radiationless decay of the primary radical pair at F_{sat} (*28*). It was shown previously that only a minor part of the quenching observed with single-turnover flashes arises from either donor side or non-heme Fe-dependent mechanisms (*23*); therefore, these two mechanisms were not considered for further analysis. In terms of the RRP model for PS II, the antenna quenching mechanism would be expressed by an increase of k_A and the decreased yield of recombination fluorescence by an increase of k_D.

As a first step (described under Global Lifetime Analysis), we analyzed fluorescence decay kinetics from all detection wavelength globally using the sum of five exponential components as a model function. The results of this analysis were used to recalculate deconvoluted PS II decay curves, which were then compared with simulated decays constructed from the kinetic model shown in Figure 5. In performing model simulations, we attempted to recover F_{sat} decay kinetics starting from the parametrized F_m curves, i.e., fluorescence time courses computed from the parameters of the kinetic model (Figure 5) by adjusting k_A, k_D, or k_{PC}^-. The results of these simulations are presented in Figure 6.

Assumption I: Variable k_D. Differences in recombination fluorescence can reasonably be considered as a possible mechanism for differences in F_{sat} and F_m as decay kinetics calculated assuming a higher rate of radiationless decay of the primary radical pair or lower rate of the back-reaction do approach the experimental decays for F_{sat}. However, even complete elimination of recombination fluorescence by setting either k_D to very large values or k_{PC}^- to zero at any PS IIα/PS IIβ ratio (Figure 6A,B) was not sufficient to account for the full extent of quenching. The inset in Figure 6 shows the relative part of the fluorescence yield increase from F_{sat} to F_m, that cannot be described by recombination, as a function of PS IIβ fraction. Irrespective of the PS IIα/PS IIβ ratio, a significant part of the fluorescence yield difference between F_{sat} and F_m cannot be modeled by an increase of radiationless deactivation of the primary radical pair. Over the reasonable range of PS IIβ fraction (30−36%), 48−56% of the difference in the fluorescence yield between F_{sat} and F_{max} cannot be accommodated by the largest possible changes in recombination fluorescence.

Assumption II: Variable k_A. To test the hypothesis of a higher degree of antenna-based nonphotochemical quenching in F_{sat} than in F_m, we attempted to fit the F_{sat} data set by varying k_A. The quality of the fit according to this model was drastically improved compared with attempts at varying k_D (Figure 6C). The best fit to the experimental F_{sat} decay kinetics was observed for k_A = 0.83 ns^{-1} when PS IIα/PS IIβ was set to 0.8 or k_A^α = 0.83, k_A^β = 0.79 when PS IIα/PS IIβ was 2. Thus, adjustment of only one parameter of the kinetic model was found to be sufficient to completely describe the difference between F_m and F_{sat} decay kinetics regardless of the assumed PS IIα/PS IIβ ratio.

As discussed earlier, we would expect antenna quenching to be similar at F_0 and F_{sat}. In our first combined kinetic analysis of F_0 and F_{sat}, k_A was assumed to be 0.3 ns^{-1}. Rate constants for kinetic analysis of F_0 and F_{sat} with k_A = 0.83 ns^{-1} are shown in Table 1. Due to the large value of k_{PC} at F_0, the rate constants are not greatly affected by the increase in k_A. At F_{sat}, the increase in k_A results in a decrease in k_{PC} and in k_{PC}^-, which brings these values much closer to those observed at F_m.

Assumption III: Variable k_{PC}, k_{PC}^-, and k_D, Fixed k_A. The time course of the fluorescence kinetics at F_m and F_{sat} can be modeled as well by assuming equal k_A values for both (F_m and F_{sat}) conditions and letting all other rate constants vary. Inspection of the data in Table 1 shows that in the case of PS IIα/PS IIβ =1 adjustment of all six remaining PS II rate constants is required to transform the kinetics of the model from F_m to F_{sat}. When PS IIα/PS IIβ = 2, the recovered $k_{PC}^{(\beta)}$ is very small, and the fluorescence decay pattern is virtually independent of the values of $k_{PC}^{-(\beta)}$ and $k_{ST}^{(\beta)}$. Therefore, there is a large error in estimation of these parameters. The physical requirements of the changes between F_m and F_{sat} based on the above changes in rate constants are an increase of the electronic coupling between P680 and Pheo and the free energy difference (ΔG) for radical pair formation (to various extents for differing PS IIα and PS IIβ fractions) accompanied with an increase (PS IIβ) or decrease (PS IIα) of k_D. These changes would imply a significant structural reorganization of the reaction center proteins and/or changes of the local electric fields. It is

unlikely that multiple turnovers of PS II would lead to such complex changes of the primary photochemistry, some of which must even be opposite in direction (k_D) for PS IIα and PS IIβ centers.

In conclusion, we found the simplest and most reasonable way to model the difference in decay kinetics between F_{sat} and F_m was to assume an increase in k_A from 0.3 ns^{-1} at F_m to 0.83 ns^{-1} at F_{sat}.

Experimental Verification of the Model Prediction. This prediction of the model can be tested experimentally: the addition of a quencher, specifically acting on the antenna, in the appropriate amount must result in transformation of decay kinetics measured after multiturnover excitation to those measured under single-turnover conditions. It is well established that exogenous oxidized quinones quench Chl fluorescence in vivo (*47*−*49*). Previously we showed that fluorescence quenching, induced by the exogenous oxidized 5-hydroxynaphthoquinone, is an antenna-based quenching that is completely described by an increase of k_A (*37*). The amount of quinone required to increase k_A from 0.3 to 0.83 ns^{-1} can be estimated using the Stern−Volmer equation:

$$k_A^{[Q]}/k_A^{[0]} = 1 + k_{SV}[Q]$$

In our previous work (*37*) on the analysis of fluorescence decay kinetics at F_0, we derived a concentration dependence of $k_A^{[Q]}$ and found that k_{SV} was equal to 1.8×10^{-5} M^{-1}. In that analysis, $k_A^{[0]}$ was set to 0.3 ns^{-1}. The results of kinetic modeling performed in the present study suggest that an intrinsic quencher causes an increase of $k_A^{[0]}$ to 0.83 ns^{-1} at F_{sat} and F_0 as compared to F_m. We therefore repeated the Stern−Volmer analysis of our previous F_0 dataset by setting the initial $k_A^{[0]}$ to 0.83 ns^{-1} and calculated a corrected $k_{SV} = 1.1 \times 10^{-5}$ M^{-1}. Using this constant, we determined the extrinsic quinone concentration required to quench F_m to F_{sat} to be [Q] = 15 μM. The sample fluorescence decay curves of thylakoids in the presence of 15 μM 5-OH-NQ measured at F_m and DAS resulting from global lifetime analysis are shown in Figure 3 and Figure 4 correspondingly. Inspection of the data readily shows that fluorescence decay kinetics and corresponding DAS measured at F_m in the presence of 5-OH-NQ and at F_{sat} without any quinone addition are very similar. Combined global analysis of fluorescence decay kinetics at F_0, F_{sat}, and $k_M^{[Q]}$ performed using the RRP model revealed a very similar set of rate constants for F_{sat} and $k_M^{[Q]}$ (Table 1). Accordingly, we can conclude that the low yield of variable fluorescence at F_{sat} arises from an enhanced antenna-based nonphotochemical quenching as compared to the F_m state.

Identification of the Quenching Species. Previous work has suggested that an oxidized nonphotochemical quencher which is gradually reduced in the course of multiple-turnover excitation of PS II is responsible for the low F_{sat} yield (*24*). The quenching species has been proposed to be either oxidized plastoquinone (*25*), an alternative quencher Q_2 (*26, 27*), or multiple structurally independent quenchers (*21, 22*). Our present work cannot distinguish between these alternatives but does localize the site of quenching to the antenna by constraining the mechanism to changes in k_A. Previous work from our laboratory has shown the absorption cross section of PS II to be decreased when PQ was oxidized, supporting a role for oxidized PQ as antenna quencher. However, in that study DCMU abolished most of the effect of PQ redox state on the cross section. F_m is also commonly obtained by illuminating thylakoids in the presence of DCMU, conditions which oxidize plastoquinone. These two results indicate that the mechanism of quenching is more complex than a direct quenching of the bulk antenna chlorophyll by oxidized plastoquinone or that DCMU somehow interferes with the quenching mechanism (*23*). Kolber et al. (*50*) have suggested that the fluorescence yield changes between F_{sat} and F_m are a result of occupancy of the Q_B binding site. Their work indicates that F_m arises when the Q_B site is empty and F_{sat} arises when the site is occupied by oxidized quinone or semiquinone. Our current results are consistent with this model if the oxidized quinone, occupying the Q_B site, acts as an antenna quencher and increases k_A.

Implications of the Change in k_A between F_{sat} and F_m on Calculations of Photochemical Quenching (q_p). F_0 and F_m are widely used to delimit the full range of variable fluorescence which can be attained by changes in photochemical quenching (q_p). At F_m, q_p is zero, and at F_0 it is maximal. A simple approximation calculation is often used to quantify q_p at any observed level of variable fluorescence (F) between F_0 and F_m.

$$q_p = (F_{m'} - F)/(F_{m'} - F_{0'})$$

Nonphotochemical quenching is defined as anything which decreases F_m to a lower level ($F_{m'}$) and in some instances decreases F_0 as well to a level $F_{0'}$. In the presence of nonphotochemical quenching, the parameters $F_{0'}$ and $F_{m'}$ are used in the calculation for q_p.

An implicit assumption in the above is that the multiple-turnover saturating light pulses used to determine F_m or $F_{m'}$ do not affect the absolute amount of nonphotochemical quenching of PS II. However, our results indicate very strongly that F_0 and F_{sat} are characterized by a greater degree of nonphotochemical quenching than F_m. The multiple-turnover flash conditions used to measure F_m decrease the total amount of nonphotochemical quenching of PS II. This means that F_m is not an accurate measure of the release of photochemical quenching alone. Measurements of F_{sat} are required to observe the release of photochemical quenching without affecting nonphotochemical quenching. Measurements of F_{sat} accurately record the total amount of nonphotochemical quenching present and vary from a minimum value in dark-adapted samples to a maximal value approaching F_m when samples are under saturating multiple-turnover conditions.

Under most physiological light conditions there is a significant difference between F_m and F_{sat}. The use of F_m or F_m' to calculate q_p thus results in a significant overestimation of photochemical quenching. Therefore, the results of our study support the proposal of (*50*) to use F_{sat} rather than F_m in quantitative calculations of q_p.

Conclusions. We have obtained picosecond time-resolved fluorescence decay kinetics for the first time from thylakoids where PS II was closed with a single-turnover flash (F_{sat}). The transition from F_0 to F_{sat} was modeled well with the RRP model by assuming a single population of PS II with the expected changes in photochemical rate constants upon

reaction center closure. In addition, we have shown that a heterogeneous population of PS II was required for kinetic modeling of the F_m state. This was mostly a result of the relatively low rate constant for excitation decay in the antenna (k_A) at F_m which allowed the observation of a population of photochemically competent but PQ nonreducing centers that were characterized by an essentially monoexponential decay kinetic.

The transition from F_{sat} to F_m was most easily modeled by a decrease in k_A. We could not model the transition by an increase in recombination fluorescence. In addition, F_m decay kinetics were converted to F_{sat} kinetics by the addition of the known antenna quencher 5-hydroxynaphthoquinone. This is all strong evidence for antenna-based nonphotochemical quenching as the origin of low fluorescence yield after a single-turnover saturating flash. We therefore propose that the origin of the "thermal" phase of fluorescence induction is the relief of this nonphotochemical quenching induced by multiple turnovers of PS II.

ACKNOWLEDGMENT

We thank the Brock electronics and machine shops for their excellent technical assistance.

REFERENCES

1. Genty, B., Briantais, J.-M., and Baker, N. R. (1989) *Biochim. Biophys. Acta 990*, 78−92.
2. Weis, E., and Berry, J. A. (1990) *Biochim. Biophys. Acta 894*, 198−208.
3. Oxborough, K., and Baker, N. R. (1997) *Photosynth. Res. 54*, 135−142.
4. Mauzerall, D., and Greenbaum, N. L. (1989) *Biochim. Biophys. Acta 974*, 119−140.
5. Ley, A. C., and Mauzerall, D. C. (1982) *Biochim. Biophys. Acta 680*, 95−106.
6. Falkowski, P. G., Wyman, K., Ley, A. C., and Mauzerall, D. C. (1986) *Biochim. Biophys. Acta 849*, 183−192.
7. Samson, G., and Bruce, D. (1995) *Biochim. Biophys. Acta 1232*, 21−26.
8. Bowes, J., and Crofts, A. R. (1980) *Biochim. Biophys. Acta 590*, 373−384.
9. Crofts, A. R., and Wraight, C. A. (1983) *Biochim. Biophys. Acta 726*, 149−185.
10. Van Gorkom, H. J., Pulles, M. P. J., Haveman, J., and den Haan, G. A. (1976) *Biochim. Biophys. Acta 423*, 217−226.
11. Bruce, D., Samson, G., and Carpenter, C. (1997) *Biochemistry 36*, 749−755.
12. Krause, G. H., and Weis, E. (1991) *Annu. Rev. Plant Physiol. Plant Mol. Biol. 42*, 313−349.
13. Renger, G. (1992) in *The Photosystems: Structure, Function and Molecular Biology* (Barber, J., Ed.) pp 45−99, Elsevier, Amsterdam.
14. Holzwarth, A. R., and Roelofs, T. A. (1992) *J. Photochem. Photobiol., B 15*, 45−62.
15. Dau, H. (1994) *Photochem. Photobiol. 60*, 1−23.
16. Strasser, R. J., Srivastava, A., and Govindjee (1995) *Photochem. Photobiol. 61*, 32−42.
17. Srivastava, A., Guisse, B., Greppin, H., and Strasser, R. J. (1997) *Biochim. Biophys. Acta 1320*, 95−106.
18. Schreiber, U., and Neubauer, C. (1987) *Z. Naturforsch. 42*, 1255−1264.
19. Trissl, H.-W., and Lavergne, J. (1994) *Aust. J. Plant Physiol. 22*, 183−193.
20. Neubauer, C., and Schreiber, U. (1987) *Z. Naturforsch. 42*, 1246−1254.
21. Valkunas, L., Geacintov, N. E., France, L. L., and Breton, J. (1991) *Biophys. J. 59*, 397−408.
22. France, L. L., Geacintov, N. E., Breton, J., and Valkunas, L. (1992) *Biochim. Biophys. Acta 1101*, 105−119.
23. Samson, G., and Bruce, D. (1996) *Biochim. Biophys. Acta 1276*, 147−153.
24. Delosme, R. (1967) *Biochim. Biophys. Acta 143*, 108−128.
25. Vernotte, C., Etienne, A. L., and Briantais, J.-M. (1979) *Biochim. Biophys. Acta 545*, 519−527.
26. Joliot, P., and Joliot, A. (1977) *Biochim. Biophys. Acta 462*, 559−574.
27. Joliot, P., and Joliot, A. (1979) *Biochim. Biophys. Acta 546*, 93−105.
28. Schreiber, U., and Krieger, A. (1996) *FEBS Lett. 397*, 131−135.
29. Schatz, G. H., Brock, H., and Holzwarth, A. R. (1988) *Biophys. J. 54*, 397−405.
30. Roelofs, T. A., Lee, C.-H., and Holzwarth, A. R. (1992) *Biophys. J. 61*, 1147−1163.
31. Wagner, B., Goss, R., Richter, M., Wild, A., and Holzwarth, A. R. (1996) *J. Photochem. Photobiol., B 36*, 339−350.
32. Vass, I., Gatzen, G., and Holzwarth, A. R. (1993) *Biochim. Biophys. Acta 1183*, 388−396.
33. Vasil'ev, S., Bergmann, A., Redlin, H., Eichler, H.-J., and Renger, G. (1996) *Biochim. Biophys. Acta 1276*, 35−44.
34. Eijckelhoff, C., and Dekker, J. P. (1995) *Biochim. Biophys. Acta 1231*, 21−28.
35. Whitmarsh, J., and Ort, D. (1984) *Arch. Biochem. Biophys, 231*, 3378−3389.
36. Zeigler, R., and Egle, K. (1965) *Beitr. Biol. Pflanz. 41*, 11−37.
37. Vasil'ev, S., Wiebe, S., and Bruce, D. (1998) *Biochim. Biophys. Acta 1363*, 147−156.
38. Hodges, M., Moya, I., Briantais, J.-M., and Remy, R. (1987) *Prog. Photosynth. Res. 86*.
39. Van Gorkom, H. J. (1987) in *Light emission by plants and bacteria* (Govindjee, Amesz, J., and Fork, D., Eds.) pp 267−289, Academic Press, Orlando.
40. Melis, A. (1991) *Biochim. Biophys. Acta 1058*, 87−106.
41. Melis, A. (1985) *Biochim. Biophys. Acta 808*, 334−342.
42. Chylla, R. A., and Whitmarsh, J. (1987) *Biochim. Biophys. Acta 894*, 562−571.
43. Jansson, S., Stefánsson, H., Nyström, U., Gustafsson, P., and Albertsson, P.-Å. (1998) *Biochim. Biophys. Acta 1320*, 297−309.
44. van Wijk, K. J., Schnettger, B., Graf, M., and Krause, G. (1993) *Biochim. Biophys. Acta 1142*, 59−68.
45. Shinkarev, V. P., and Govindjee (1993) *Proc. Natl. Acad. Sci. U.S.A. 90*, 7466−7469.
46. Diner, B. A., and Petrouleas, V. (1987) *Biochim. Biophys. Acta 895*, 107−125.
47. Seely, G. (1978) *Photochem. Photobiol. 27*, 639−654.
48. Karukstis, K., Birkeland, K., Babusis, B., Kasal, K., and Jewell, C. (1992) *J. Lumin. 51*, 119−128.
49. Lee, J. W., Zipfel, W., and Owens, T. G. (1992) *J. Lumin. 51*, 79−85.
50. Kolber, Z. S., Prasil, O., and Falkowski, P. G. (1998) *Biochim. Biophys. Acta* (in press).
51. Wasielewski, M. R., Johnson, D. G., Seibert, M., and Govindjee (1989) *Proc. Natl. Acad. Sci. U.S.A. 86*, 524−528.

BI9806854